Emilija Zdraveva,[1] Zenun Skenderi,[2] Ivana Salopek Čubrić,[2] Budimir Mijovic[1]
[1] University of Zagreb Faculty of Textile Technology, Department of Fundamental Natural and Engineering Sciences, Prilaz b. Filipovića 28a, Zagreb, Croatia
[2] University of Zagreb Faculty of Textile Technology, Department of Textile Design and Management, Prilaz b. Filipovića 28a, Zagreb, Croatia

Effects of Morphology, Structure and Altering Layers on the Composite Heat Resistance of Electrospun PS/PU

Vpliv morfologije, strukture in razporeditve elektropredenih plasti iz PS/PU na toplotni upor kompozita

***Original scientific article**/Izvirni znanstveni članek*
Received/*Prispelo* 7–2024 • Accepted/*Sprejeto* 12–2024

Corresponding author/*Korespondenčna avtorica:*
Assist. Prof. Emilija Zdraveva, PhD
Tel: +38513712557
E-mail: emilija.zdraveva@ttf.unizg.hr
ORCID iD: 0000-0003-2845-8630

Abstract

Thermal insulating materials are of paramount importance in many application areas, including building construction, electronics, aerospace engineering, the automobile industry and the clothing industry. Electrospun materials are light weight with a well-controlled fibre diameter/morphology and a highly interconnected porous structure that facilitates the trapping of air and breathability. When combined with other conventional materials, they enhance the thermal insulating property of a composite structure. This study focused on electrospun single polyurethane (PU), polystyrene (PS) and layered composites thereof, in terms of heat resistance and its dependence on fibre diameter, pore area, number, thickness (solution volume) and the position of electrospun layers. It thus contributes to the field by addressing the effects of multiple parameters effect on a composite material's heat resistance. The fibre diameter for both electrospun polymers increased significantly by increasing the concentration, while there was a generally opposite effect from increasing electrical voltage. The 10 wt% PU and 30 wt% PS used to produce the layered composites demonstrated the highest reduction of the fibre mean diameter, from (443 ± 224) nm to (328 ± 148) nm, and from (2711 ± 307) nm to (2098 ± 290) nm, respectively. Thicker PS fibres resulted in the greatest mean pore areas of (13 ± 9) μm^2, while the PU mean pore areas were in the range of (2 ± 1) μm^2 to (4 ± 2) μm^2. Although all single and PS/PU composites demonstrated a porosity greater than 97%, their configuration in terms of number of layers, total thickness and PS and PU positioning (includes fibre diameter and pore area) affected the measured heat resistance. Single electrospun PS demonstrated a reduction in heat resistance of 0.0219 m^{2}K/W (compared to electrospun PU) due to its thicker fibres and larger pore areas, and thus looser structure. Combining the two electrospun layers improved heat resistance up to 0.0341 m^{2}K/W. The total heat resistance of the layered PU/PS composite was increased (up to 0.1063 m^{2}K/W for the electrospun PS/PS/PU/PU) by increasing the number and volume of each electrospun layer solution, and by spinning the PU layer on top of the system, which resisted the heat flow due to its smaller pore areas and

compact structure. These results prove that by optimizing process/structure parameters, a multi-layered material with good thermal performance can be designed to meet the requirements of a thermal insulating product.
Keywords: polyurethane, polystyrene, fibre diameter, pore area, thermal resistance

Izvleček

Toplotnoizolacijski materiali so izjemno pomembni na številnih področjih uporabe, vključno z gradbeništvom, elektroniko, vesoljskim inženiringom, avtomobilsko in oblačilno industrijo. Elektropredeni materiali so lahki, iz vlaken enakomerne debeline/morfologije in visoke medsebojne povezanosti v porozno strukturo, ki zagotavlja zadrževanje zraka in dihalnost. S kombiniranjem elektropredenih s klasičnimi materiali v kompozitne strukture se izboljša toplotna izolativnost. V raziskavi sta proučevana vpliv premera vlaken in površine por na toplotni upor enoplastnih poliuretanskih (PU) in polistirenskih (PS) elektropredenih materialov in vpliv števila, debeline (volumna raztopine) in položaja elektropredenih plasti v večplastnih kompozitnih strukturah, saj vsi omenjeni parametri vplivajo na toplotni upor kompozitnega materiala. Pri obeh elektropredenih polimernih materialih se je debelina vlaken znatno povečala z naraščajočo koncentracijo predilne raztopine, pri čemer je zviševanje električne napetosti na splošno vplivalo na zmanjševanje debeline vlaken. Pri večplastnih kompozitnih materialih, izdelanih z uporabo raztopin 10 ut.% PU in 30 ut.% PS, je bilo z naraščajočo električno napetostjo zmanjšanje povprečne debeline vlaken najbolj izrazito, s (443 ± 224) nm na (328 ± 148) nm in z (2711 ± 307) nm na (2098 ± 290) nm. Materiali iz najdebelejših vlaken iz PS so imeli največje povprečne površine por (13 ± 9) μm^2, medtem ko so bile povprečne površine por materialov iz PU v razponu od (2 ± 1) μm^2 do (4 ± 2) μm^2. Čeprav so vsi enoplastni in večplastni PS/PU-kompoziti dosegli več kot 97-odstotno poroznost, pa je njihova konfiguracija – število plasti, skupna debelina in položaj PS in PU (vključuje premer vlaken in površino por) – vplivala na izmerjeni toplotni upor. V primerjavi z elektropredenim PU je enoplastni elektropredeni PS material zaradi debelejših vlaken in večje površine por dosegel za 0,0219 m2K/W nižji toplotni upor, imel je bolj zrahljano strukturo. Kombinacija dveh elektropredenih plasti je izboljšala toplotni upor do 0,0341 m^{2}K/W. Skupni toplotni upor večplastnega PU/PS-kompozita se je povečal – na 0,1063 m^{2}K/W za elektropredeni PS/PS/PU/PU – s povečanjem števila plasti in uporabljenega volumna predilnih raztopin ter s PU-plastjo na zunanji strani kompozita, ki je zaradi manjše površine por in kompaktnejše strukture imela višji toplotni upor. Ti rezultati dokazujejo, da je mogoče z optimizacijo procesnih in strukturnih parametrov oblikovati večplastni kompozitni material z lastnostmi, ki ustrezajo zahtevam toplotnoizolacijskega izdelka.
Ključne besede: poliuretan, polistiren, premer vlakna, površina pore, toplotni upor

1 Introduction

Thermal insulation is extremely important in many applications that require a balance of temperature or protection against temperature fluctuations. There are many natural materials (e.g. wool, fur, feathers, wood fibres, expanded cork, cotton, flex, hemp and reed), [1–3] that are good thermal insulators with a high heat resistance used in the areas of building construction [4], electronics, aerospace engineering, the automobile industry [5] and the clothing industry [6]. Besides natural, frequently used artificial insulating materials include asbestos, rock wool, fibre-glass, expanded clay, perlite and plastic foams (i.e. polystyrene, polyurethane, polyester) [7]. Today, advanced materials and the associated technologies have become a prerequisite in the development of thermally insulating materials that will fulfil the requirements of a modern product. These include low thermal conductivity, chemical and physical stability at high operating temperatures, mechanical integrity, non-toxicity and more, specifically, fire, water and pest resistance, lightweight, porous structure, durability, cost-effectiveness and sustainability. High-per-

formance materials for thermal insulation do not necessarily mean the use of manmade materials, such as plastics or composites thereof (i.e. with organic or inorganic based additives), but also natural-based materials from renewable resources, such as by-products or waste (e.g. seagrass, palm fibres, cornstalks and rice husks) from agriculture or other industries [3]. Recent advanced technologies that have emerged as promising in this field include 3D printing [8] and various nanostructure fabrication techniques (e.g. electrospinning) [9]. The 3D printing technique offers versatility in material composition (e.g. polymers, ceramics and metals), flexibility in design, and custom shaping with complex cellular geometries and dimensions [10]. The technique of electrospinning facilitates the fabrication of lightweight nanofibrous materials with a large surface area, high porosity and interconnected pores with the ability to entrap a large quantity of air in between as an extremely important property in thermal performance. The process utilizes electrostatic forces that stretch a viscoelastic polymer solution to form ultrathin fibres that are solidified as the jet reaches a collector after organic solvent evaporation [11]. Fibre diameter, morphology and the pore sizes of electrospun materials are very well-controlled through the adjustment of a polymer solution's properties, processing parameters and ambient conditions. The crucial parameter that affects fibre uniformity is the polymer solution concentration, which is directly related to its viscosity, while higher solution viscosity results in thicker fibres [12]. Increasing a solution's concentration prevents partial jet break up due to higher viscoelastic force, as well as increased polymer chain entanglement, that results in the formation of smooth, uniform fibres [13]. The most dominant processing parameter that affects fibre diameter and morphology is electrical voltage. Generally, increasing electrical voltage reduces fibre diameter due to an increase in the stretching force. Opposite observations have also been reported, as well as no significant changes in fibre diameter [14–16]. Among the many application areas that are well-known for these materials (e.g. biomedicine, electronics, energy storage and conversion, environmental protection, chemistry and functional textiles [11]), the field of thermal insulation is explored to a lesser extent. The advantages of electrospun materials over conventional materials include their light weight, the ability to control fibre diameter/morphology, and their highly porous structure, which facilitates the trapping of air and breathability. These materials perform better in terms of heat resistance when combined with other conventional materials, i.e. in a composite structure. Some of the first reported studies concern a comparison of electrospun polyacrylonitrile (PAN) thermal performance to commercially available insulation materials, such as waterfowl down and wool, high-loft polyester (artificial down, Primaloft), meltblown pitch carbon fibre and silica aerogel-impregnated flexible fibrous insulation. The authors concluded that electrospun PAN may be used in hybrid battings, meaning nanofibers can be incorporated into existing insulating materials to improve thermal insulation, while microfibers are needed for durability and compression recovery [9]. Major factors influencing thermal insulation efficiency also include fibre diameter, added particles and structures density in a thermal insulating composite. Single nozzle and co-axial electrospinning were performed for the fabrication of PAN/silica aerogel laminated composites, where the latter showed a reduction in thermal conductivity by 12.5%. When a spacer layer of hollow glass microspheres were inserted in the composite structure, insulation improved by 20% [17]. More complex electrospun structures were prepared using modified twisting yarn electrospinning. Continuous hollow yarns with phase changeability were fabricated from hydroxypropyl cellulose-based mixed esters and poly (m-phenylene isophthalamide) (HPCMEs/PMIA). The yarns demonstrated a heat storage capacity of 20–30 kJ/kg and an air coupling ability, and can thus be used in thermal regulation and thermal insulation applications [18]. Polystyrene (PS) and polyurethane (PU) are frequently used polymers in the building insulation market, as they are low in cost and have low thermal conductivities due to

their foam microstructures [19]. Improved super-insulating materials (with greatly reduced thermal conductivity) are usually obtained when the same are combined with nanofillers in a composite system [20].

To best of our knowledge, few studies address the heat resistance properties of electrospun materials and the measurement thereof using a sweating guarded hot plate. In fact, we report here on only one study (found in available literature) where a sweating hotplate device was used to measure the heat resistance of multi-jet electrospun polystyrene/polyamide 6 (PS/PA 6). The material demonstrated lowered thermal resistance due to the higher thermal conductivity and lowered air content of the compact PA 6. When electrospun in a higher humidity environment, PS generated more pores and a rougher surface, and thus demonstrated higher heat resistance. It has been suggested that the system be used as thermally comfortable textile [21]. Other authors reported on the water vapour resistance evaluation of electrospun polyacrilonitrile (PAN) using the Permetest skin model. The study showed an exponential correlation between water vapour resistance and the membrane ratio: varying the morphology of the electrospun PAN resulted in a water vapour permeability value of between 0.1 Pam²/W and greater than 10 Pam²/W [22]. This study considered electrospun single and composite PS/PU microporous materials to be used in thermal protective applications (i.e. protective clothing or aids). The effect of the processing parameters (electrical voltage and polymer solution concentration) on fibre morphology, the number of electrospun layers, thickness (solution volume) and their consecutive position on the composite heat resistance were examined.

2 Experimental part

2.1 Materials and methods

The polymers used in this study were polyurethane (PU), DESMOPAN 588E produced by Bayer, Germany, and polystyrene (PS) 678E, produced by Dioki, Croatia, and organic solvents N,N-dimethylformamide (DMF) and tetrahydrofuran (THF), produced by Sigma Aldrich. The textile substrate used to support the electrospun material was a commercially available fine woven net textile (polyamide tulle). The PU was of extrusion and injection moulding grade with improved microbial and hydrolysis resistance and a density of 1.15 g/cm³. The PS was general purpose, transparent, with excellent optical properties, processability, high melt flow rate and a density of 1.05 g/cm³. The two polymers were dissolved in DMF/THF and DMF (weight ratio of 2:3) to prepare two separate ranges of solutions 10–16 wt% and 24–30 wt% for the PU and PS, respectively. Electrospun materials were produced by electrospinning device type NT-ESS-300, NTSEE Co. Ltd., South Korea. The processing conditions, electrical voltage *U* (kV), needle tip to collector distance x (cm) and volume flow rate v (mL/h) are presented in Table 1, while the collector rotation speed was 90 rpm and the collector horizontal migration was 0.206 m/min. These conditions refer to electrospun materials used to evaluate a material's morphology and porosity.

Table 1: Electrospinning process conditions

Polymer	Parameters			
	c [a] (wt%)	*U* [b] (kV)	*v* [c] (mL/h)	x [d] (cm)
Polyurethane	10, 12, 14, 16	10, 12, 14, 16, 18	1	12
Polystyrene	24, 26, 28, 30	10, 12, 14, 16, 18, 20	1–4	12

[a] concentration, [b] voltage, [c] volume flow rate, [d] needle tip to collector distance

For the purpose of heat resistance evaluation, the materials were fabricated (dimensions of 30 cm x 30 cm) using a single or combined PS and PU electrospinning solution on a net textile substrate

(NTS). PS/PU composite materials were electrospun continuously in a layer-by-layer manner. The electrospinning conditions chosen for the PU were 10 wt%, 18 kV, 12 cm and 1 mL/h, while the conditions for PS were 30 wt%, 18 kV, 12 cm and 4 mL/h. The configurations of the electrospun materials in terms of polymer solution volume and layer alteration are given in Table 2.

Table 2: Electrospun single and composite materials configurations

Sample ID	A	B	C
	V = const (4 mL (total))	$V \neq$ const (4 mL each layer)	$V \neq$ const (4 mL each layer)
1	PU; one layer (A = B = C)		
2	PS; one layer (A = B = C)		
3	PS/PU two layers	PS/PU two layers (B = C)	
4	PS/PU/PS/PU four layers	PS/PU/PS/PU four layers	PS/PS/PU/PU four layers
5	PS/PU/PS/PU/PS/PU six layers	/	/

In case of equal polymer layering, electrospinning was continued after one hour of drying at room temperature. Figure 1 illustrates the configurations of the three types (A, B and C) of single and PS/PU composite materials. "A" stands for materials/composites made from one, two, four or six PS and PU alternating layers with a total polymer solution volume of 4 mL. Materials in group A were made from one layer (PS or PU), two layers electrospun one by one (PS/PU), four (PS/PU/PS/PU) or six alternating layers PS/PU/PS/PU/PS/PU. The difference between group A and B was in the polymer solution volume.

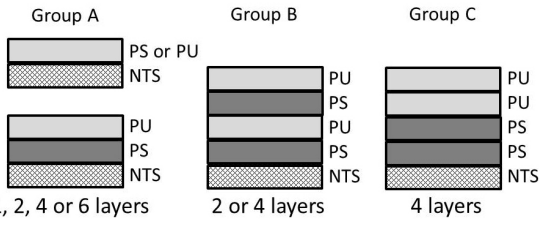

Figure 1: Scheme of the electrospun PS and PU alternating layers

"B" stands for materials/composites made from one, two or four PS and PU alternating layers with a polymer solution of 4 mL for each single layer. "C" stands for materials/composites made from one, two or four PS and PU repeating layers with a polymer solution of 4 mL for each single layer. The difference between group B and C is in the electrospinning order of the polymers, as seen in Figure 1. For all composites, the top layer of each configuration was PU, as it facilitates better adherence, due to faster solvent evaporation, in contrast to the high PS concentration solution system. To ensure composites compactness, each of the configurations was electrospun on a net textile substrate.

2.1.1 SEM analysis and porosity calculation

The morphology of the electrospun materials was observed using a SEM MIRA3 TESCAN scanning electron microscope, with palladium/gold coating beforehand. The fibre diameter and pore area were measured using randomly selected 100 fibres, while areas between the fibres were measured using *ImageJ* software. A statistical analysis of the collected data was performed using OriginLab software. ANOVA and Tukey tests were conducted taking into account comparisons that were statistically significant at $p < 0.05$.

The thickness of the electrospun materials was measured on a reconstructed universal measuring

microscope with a laser interferometer connected to a computer, Carl Zeiss (resolution of 0.0001 mm), University of Zagreb Faculty of Mechanical Engineering and Naval Architecture. The porosity P (%) of the single (P_s) and composite (P_c) electrospun materials was estimated using equations 1 and 2, respectively [23].

$$P_s = (1 - \frac{\frac{m}{A \cdot h}}{\rho_p}) \cdot 100\% \quad (1)$$

$$P_c = (1 - \frac{\frac{m_{c1}}{\rho_{c1}} + \frac{m_{c2}}{\rho_{c2}}}{V_c}) \cdot 100\% \quad (2)$$

where, m (g) represents the sample mass, A(cm^2) represents the area and h(cm) represents the thickness, ρ (g/cm^3) represents the density of the polymer and V_c(cm^3) represents the composite material volume. The subscripts c_1 and c_2 refere to each of the components in the electrospun composite material.

2.1.2 Heat resistance measurement

The heat resistance of the electrospun materials was measured on a sweating guarded hotplate (SGHP) device placed in an air conditioned chamber. The hotplate simulated the transfer of heat from the skin, trough the material, to the environment by maintaining a temperature of (35 ± 0.1) °C at its surface (i.e. the human skin temperature). The conditions of the chamber were as follows: temperature of 20 °C, relative humidity of 65% and airflow velocity of 1 m/s [24]. The heat resistance ($R_{ct,}$ m^{2}K/W) of the electrospun materials was calculated according to equation 3 [25].

$$R_{ct} = \frac{(T_m - T_a) \cdot A}{H} \quad (3)$$

where, T_m (K) represents the plate temperature, T_a (K) represents the air temperature, and H/A (W/m^2) represents the heat flux.

3 Results and discussion

Figures 2–4 show the SEM images of the single electrospun PU (10–16 wt%) and PS (24–30 wt%) materials, PS/PU composite materials, and the associated textile substrate in the composite configurations. The PU electrospun fibres showed variations in the thicknesses along their lengths with random beads, especially in the case of 10 and 12 wt% solutions (Figure 2a–2b). An increase in the PU polymer concentrations (above 10 wt%; see Figure 2b–2d), resulted in an increase in the fibres' uniform morphology, i.e. the fibres had circular cross sections, no deformations along the length and smooth surfaces.

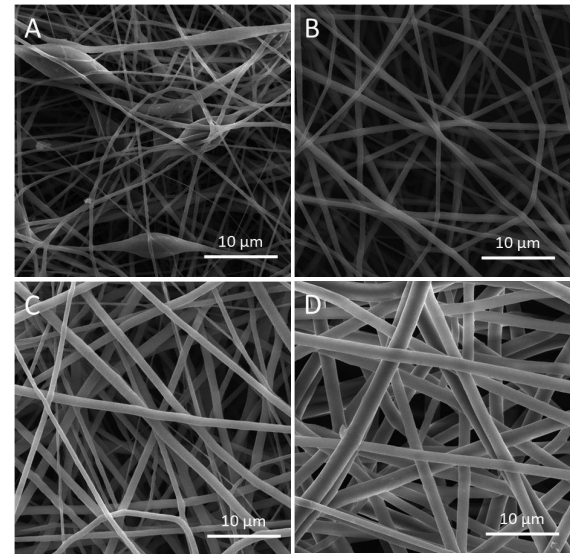

Figure 2: Electrospun single PU in concentrations of: a) 10 wt%, b) 12 wt%, c) 14 wt% and d) 16 wt% (supplemental SEM images of electrospun PU under all processing conditions presented in Table 1)

In case of the electrospun PS materials (Figure 3a–3d), the fibres demonstrated uniformity for all concentration ranges, as the latter were initially high (above 24 wt%). Thus, at higher concentrations, the solidification process of the fibres was faster because solution viscosity was predominant over surface tension, which resulted in fewer beads or in beadless fibres [26]. The SEM images clearly show the difference in the PU and PS fibres thicknesses, and

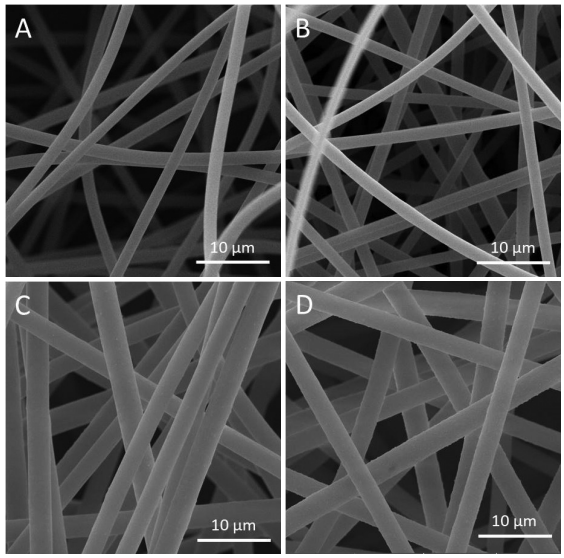

Figure 3: Electrospun single PS in concentrations of: a) 24 wt%, b) 26 wt%, c) 28 wt% and d) 30 wt% (supplemental SEM images of electrospun PS under all processing conditions presented in Table 1)

thus the composite structure (Figure 4a) illustrates the composite system with thinner PU and thicker PS fibres. Such nano/micro fibrous structures are of paramount importance in the field of biomedicine as such structures will provide cells penetration (micro pores) and free delivery, and the diffusion of nutrients as well as waste products (nano fibres) [27]. Layered systems (combining electrospun materials and conventional fabrics) will attain barrier/transport properties with different levels of thermal comfort and protection not achievable with existing personal protective materials [28]. In this study the bottom layer of the composites was a net textile substrate (Figure 4b) that will only mechanically support the electrospun materials due to its high open structure.

Figure 5 and 6 illustrate the dependence of the fibre diameter of single electrospun PU and PS on the electrical voltage and polymer solution concentrations. Generally, an increase in the electrical voltage from 10 kV to 20 kV resulted in a reduction of the fibre diameter in both polymers, which is in line with other reported studies [29]. Thinner fibres

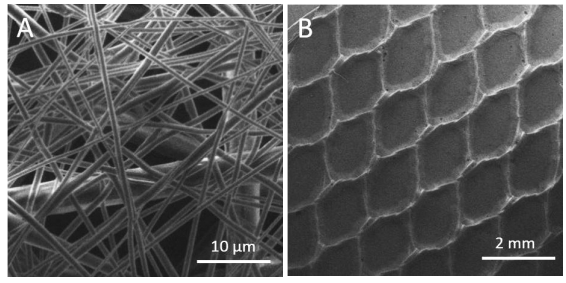

Figure 4: Electrospun materials: a) PS/PU configuration – top layer and b) PS/PU configuration – bottom layer or net textile substrate

are formed due to the increase in the charge density on the jet surface and increase in the repulsive force [30]. An opposite effect was observed in the case of the electrospun 24 wt% and 26 wt% PS at the critical voltages of 20 kV and 12 kV (Figure 6). This was also reported in the case of electrospun PU, where the diameter demonstrated a sigmoidal increase with an increase in voltage [31]. Jet traveling time was affected by an increase in electrical voltage, which then resulted in an increase in fibre diameter [32]. The concentration of 16 wt% PU was not spinnable at the voltages of 16 kV and 18 kV, while the concentration of 14 wt% PU was not spinnable at 18 kV. In the case of the electrospun PS, fibre formation was not possible in the case of the concentrations of 26 wt% and 30 wt% at the voltages of 14–20 kV and 18–20 kV, respectively. Spinnability mainly depends on the solution concentration. Thus at higher concentrations, the solvent evaporates at the tip of the needle with no possibility of the solution jet being stretched up to the collector to form the fibres. An excessively high polymer concentration and excessively high voltage will also result in a difficult spinning process [30]. The reduction of the 10 wt% PU fibre diameter with an increase in the electrical voltage was significant at voltages of 10 kV, 12 kV, 14 kV and 18 kV, and at 14 kV and 16 kV, with the highest reduction of (443 ± 224) nm to (328 ± 148) nm (Figure 5). In the case of the 12 wt% PU, the fibres were significantly thinner (highest reduction of almost 50%) for all *U* (kV) increases, except at 16 kV and 18 kV (Figure 5).

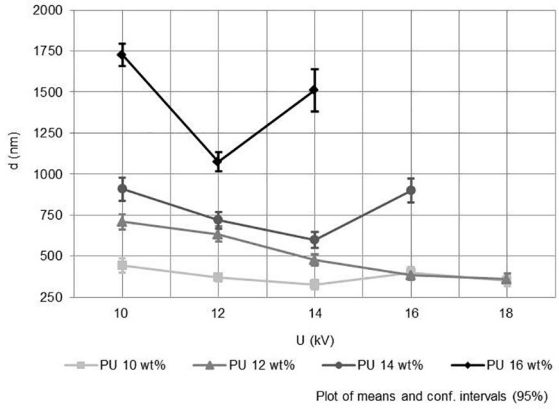

Figure 5: Effect of the concentration and electrical voltage on the electrospun PU fibre diameter

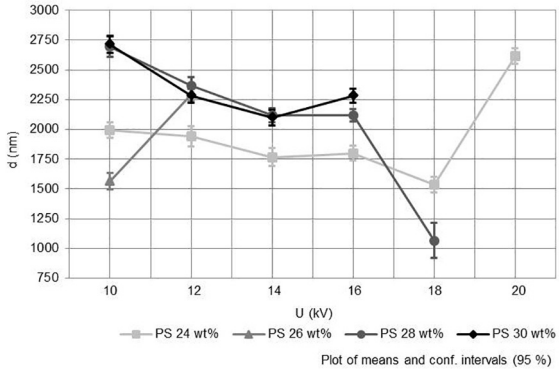

Figure 6: Effect of the concentration and electrical voltage on the electrospun PS fibre diameter

Similarly, no significant difference in the reduced fibre diameter was recorded for the 14 wt% PU at a voltage of between 10 kV and 16 kV, with the highest reduction of (908 ± 356) nm to (598 ± 238) nm. For the 16 wt% PU, a significant fibre reduction was present at all *U* (kV) levels, with the most significant reduction of more than 650 nm. Significant increases in fibre diameters were observed for the 14 wt% and 16 wt% PU, from (598 ± 238) nm to (898 ± 368) nm (14 kV to 16 kV), and (1075 ± 294) nm to (1511 ± 653) nm (12 to 14 kV), respectively (Figure 5). The trend of PS fibre diameter reduction was significant for all polymer concentrations at all increasing electrical voltage levels, except at 12 kV and 16 kV (24 and 30 wt% PS), 14 kV and 16 kV (24 wt% and 28 wt% PS). The most significant reduction in the PS fibre diameter was from (2694 ± 367) nm to (1065 ± 622) nm in case of the 28 wt% PS at the 18 kV, while the highest increase was from (1534 ± 278) nm to (2614 ± 282) nm, at the highest electrical voltage level of 20 kV for the 24 wt% PS (Figure 6). A significant increase in fibre diameter was also observed for the 26 wt% PS from (1564 ± 290) nm to (2295 ± 259) nm (10 kV to 12 kV; see Figure 6). The greatest fibre mean diameter was observed in the case of the 30 wt% PS, while the most significant reduction for that sample was from (2711 ± 307) nm to (2098 ± 290) nm at 18 kV. Figure 7 and 8 show the dependence of the single electrospun PU and PS pore area on the electrical voltage and polymer solution concentrations. Although a general reduction in the pore areas was observed with an increase in the electrical voltage, the opposite effect was also seen at certain concentrations and *U* (kV) levels. There was a higher variation of the measured values as compared to the measured fibre diameters. Studies report on the broader fibres distribution, which may influence broader pore size distribution due to enhanced jet instability caused by the high electrical voltage [33]. A reduction in fibre diameters usually results in a decrease in pore areas as well, as the pore size and its distribution depends on the fibre diameter [34].

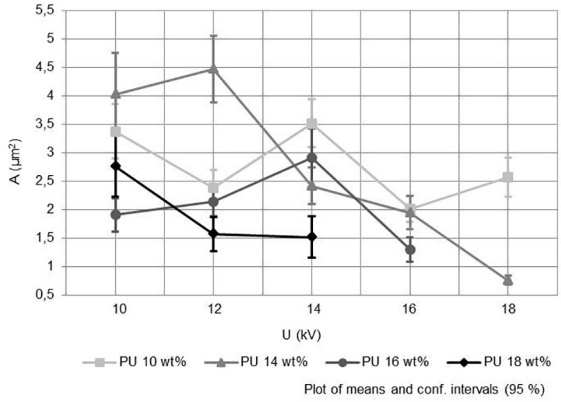

Figure 7: Effect of the concentration and electrical voltage on the electrospun PU pore area

The reduction of the 10 wt% PU pore areas with an increase of the electrical voltage was significant at voltages of 10 kV, 12 kV, 16 kV and 18 kV, 12 kV and

14 kV (pores were increased by 1.13 μm²), and at 14 kV, 16 kV and 18 kV (pores were increased by 0.55 μm² from 16 kV to 18 kV), with the highest reduction of (3.37 ± 2.43) μm² to (2.02 ± 1.16) μm² (Figure 7). In the case of the 12 wt% PU, the pore areas were significantly smaller (highest reduction of almost 3.71 μm²) for all *U* (kV) increases, except at 10 and 12 kV (pores were increased by 0.44 μm²), and at 14 kV and 16 kV (Figure 7).

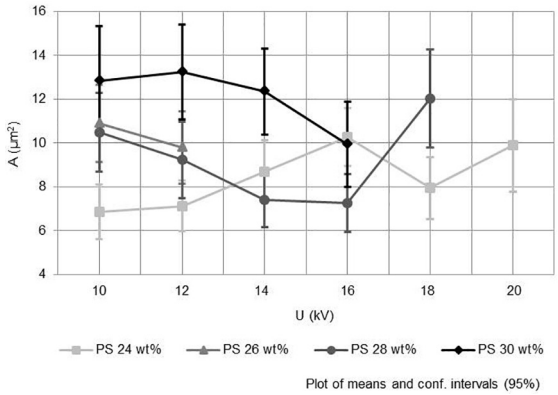

Figure 8: Effect of the concentration and electrical voltage on the electrospun PS pore area

The reduction of the pore areas in the case of the 14 and 16 wt% was only insignificant at voltages of 10 kV, 12 kV and 16 kV, and at 12 kV and 14 kV, respectively. The highest observed reductions of the pore areas were 55% (for the 14 wt% PU) and 45% (for the 16 wt% PU; see Figure 7). The variations of the measured pore areas were greater for the electrospun PS than for the electrospun PU. Thus a significant increase or reduction in pore areas was only observed in the case of the 24 wt% at voltages of 10 kV and 16 kV, and at 12 kV and 16 kV, and in the case of the 28 wt% at voltages of 14 kV and 18 kV, and at 16 kV and 18 kV (Figure 8). The most significant increase in the pore areas in the case of the 24 wt% was from (6.85 ± 5.98) μm² to (10.27 ± 6.63) μm², and from (7.26 ± 5.87) μm² to (12.03 ± 9.63) μm² in the case of the 28 wt% PS (Figure 8). In the case of the 30 wt% PS, the ranges of the mean pore areas were between (9.94 ± 8.21) μm² and (13.23 ± 9.30) μm², with the highest value observed.

Table 3 presents the electrospun materials' mass per surface area m (g/cm²), thickness *h* (mm) and calculated total porosity *P* (%). The mass per surface area and the thicknesses of the electrospun materials increased with an increase in the number of electrospun layers in the composite systems. There was no significant difference between the composite materials in terms of calculated porosity, as all of the listed materials showed porosities higher than 97%, which is quite high and beneficial, and will thus contribute to their excellent moisture vapor transport properties [35].

Table 3: Calculated porosity of electrospun materials

Sample	*m* (*10⁻³g/cm²)	*h* (mm)	*P* (%)
TS	1.08	0.1900	/
A1	0.24	0.3104	99.1
A2	0.78	0.2749	99.2
A3	0.57	0.4866	97.2
A4	0.69	0.5454	98.6
A5	0.89	0.5564	98.4
B3	1.17	0.9364	98.7
B4	2.62	0.7200	99.9
C4	2.43	1.1817	98.0

Figure 9 illustrates the heat resistance vs. thickness and vs. total porosity of single electrospun PS and PU (on the NTS), as well as the associated PU/PS/NTS composite systems with a varying number and position of layers. When observing group A of the electrospun materials, it can be easily concluded that the single electrospun PS (A2) showed reduced heat resistance (for 0.0219 m²K/W) compared to the single electrospun PU (A1) material due to thicker fibres and greater pore areas, meaning a looser structure. When the two were combined into two to six layers, the heat resistance increased up to 0.0557 m²K/W for the electrospun A5 or PS/PU/PS/PU/PS/PU material. In group B, an increase in the polymer solution volume (4 mL) in each of the consecutive layers drastically increased the composites' heat resistance to 0.0834 (B3 two layers) and 0.102 m²K/W (B4 four layers).

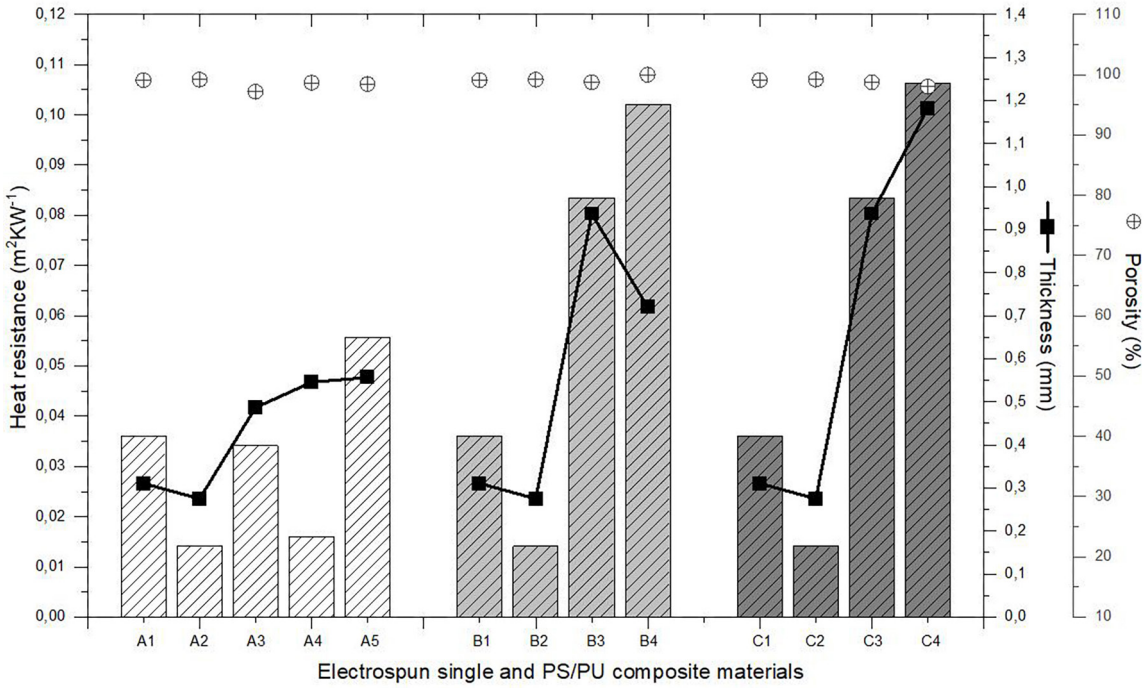

Figure 9: Heat resistance of the three groups (A, B and C) of electrospun composite materials vs. thickness and vs. porosity

The highest heat resistance of 0.1063 m^2K/W was measured for the four layered PS/PS/PU/PU (C4) composite material. When compared to the four layered B4 composite, it can be concluded that the position of the PU layer in C4 contributed to an increase in heat resistance. Two of the PU layers were electrospun as the top layers (after the two PS layers), while the reason for the increase was their small pore areas and compact structure resisting the heat flow. A previous study reported on the fabrication of a multi-layered fabric combining cotton and lyocell fabrics, and a PU nanofibrous coating to improve wind-resistance and comfort properties of knitted structures [36]. Similarly, when electrospun polyacrylonitrile (PAN) was placed between polyethylene (PE) nonwoven layers, PAN with thinner fibres (108 nm) and a higher surface density (5 g/m^2) resulted in a reduction in thermal conductivity and improved water vapor transfer by 28% [37]. When these results are correlated to the calculated total porosity, there is no trend to be followed, as the changes in the porosities among all materials were insignificant. In the case of the thickness relation, one general observation is that higher heat resistances is the result of an increase in the composite thickness (i.e. from 0.5454 mm for A4, to 0.7200 mm for B4, to 1.1817 mm for C4). A linear relationship between a fabric's heat resistance and its corresponding thickness was reported in a study of polyester knitted fabrics to provide thermal comfort in clothing design. As explained, the still air entrapped between the fibre spaces increases the heat resistance value [38]. In this study, there was the opposite effect of increasing thickness, as well. If one observes material A3 and A4, it is evident that, despite the increase in the thickness by 0.0588 mm, the heat resistance of the thicker material A4 was reduced by 0.0181 m^2K/W. This may suggest that an increase in the number of PS layers that have a looser structure or larger pore areas facilitate the pass through of heat, resulting in reduced thermal insulation. The same effect can be

seen for the B3 and B4 materials. A study reported on the evaluation of the heat resistance of different twill woven fabrics used in sportswear. The thicknesses of the fabrics were in the ranges of 0.17 mm to 0.28 mm. The measured thermal resistances were between 0.0059 m^2K/W to 0.0142 m^2K/W [39]. The single electrospun PS material in our study, with a thickness of 0.2749 mm, was comparable with the reported twill woven fabric, with a thickness of 0.28 mm. However, in terms of R_{ct}, the heat resistance of our material was 0.0139 m^2K/W higher. Similarly, another study reported the heat resistances of single jersey knitted fabrics (cotton, or cotton + elastane, grey or finished) in the ranges of ~0.015 m^2K/W to ~0.02 m^2K/W [40]. Comparing the results, one can observe the similarity of the knitted fabrics with some of those from the current study's group A materials, while increasing solution volume (material thickness), the number of layers, and the electrospinning order thereof (groups B and C) resulted in more than 0.05 m^2K/W R_{ct} (i.e. material C4, PS/PS/PU/PU, 1.1817 mm, 0.1063 m^2K/W). This suggests that the layering configuration of the electrospun materials is beneficial for thermal performance and thus would imply a combination with other conventional materials, as well. Their light weight would still not be compromised in the case of a greater number of electrospun layers, which would contribute to total comfort in terms of freedom of movement.

4 Conclusion

Among the many application areas of the electrospun materials, the field of thermal protective fabrics has been explored very little. This study deals with this topic by first investigating the effect of the electrical voltage and polymer concentrations on fibre diameter and pore area, and then by correlating the two parameters with heat resistance properties. Heat resistance, which is directly related to the material heat insulation, was measured to determine a change in heat resistance in terms of the number, thickness (solution volume) and position of electrospun layers variation in a PU/PS/NTS composite system. Generally, the higher the electrical voltage was, the thinner the PU and PS fibres were, with a few opposite effects indicating polymer jet instabilities. The electrospun PS demonstrated thicker fibres (> 1000 nm to ~2700 nm) and larger pore areas (> 6 μm^2 to ~13 μm^2), resulting in a looser structure and, as expected, in a lower heat resistance of 0.0141 m^2K/W compared to the PU of 0.036 m^2K/W. The compact structure of the electrospun PU was the result of its thinner fibres (~300 nm to ~1700 nm) and smaller pore areas (0.75 μm^2 to 4.5 μm^2), and thus improved the heat resistance of PU/PS composites. Increasing the number of electrospun layers from one to six and the volume of each electrospun layer solution, and adding a PU layer on top of the system increased the total heat resistance of the multi-layered composites, with the highest value (0.1063 m^2K/W) recorded for the group C.

Acknowledgement

This work was supported by the University of Zagreb, Faculty of Textile Technology under short-term financial support for research for 2023, TP20-23, PI: Emilija Zdraveva.

Conflict of interest statement

The authors declare there were no conflicts of interest.

References

1. FAN, M., FU, F. Introduction: a perspective–natural fibre composites in construction. In *Advanced High Strength Natural Fibre Composites in Construction*. Edited by M. Fan and F. Fu. Cambridge : Elsevier, 2017, 1–20, doi: 10.1016/B978-0-08-100411-1.00001-7.

2. KORJENIC, A., PETRÁNEK, V., ZACH, J., HROUDOVÁ, J. Development and performance evaluation of natural thermal-insulation materials composed of renewable resources. *Energy and Buildings*, 2011, **43**(9), 2518–2523, doi: 10.1016/j.enbuild.2011.06.012.
3. BOZSAKY, D. Nature-based thermal insulation materials from renewable resources. A state-of-the-art review. *Slovak Journal of Civil Engineering*, 2019, **27**(1), 52–59, doi: 10.2478/sjce-2019-0008.
4. CETINER, I., SHEA, A.D. Wood waste as an alternative thermal insulation for buildings. *Energy and Buildings*, 2018, **168**, 374–384, doi: 10.1016/j.enbuild.2018.03.019.
5. CAI, Z., AL FARUQUE, M.A., KIZILTAS, A., MIELEWSKI, D., NAEBE, M. Sustainable lightweight insulation materials from textile-based waste for the automobile industry. *Materials*, 2021, **14**(5), 1–20, doi: 10.3390/ma14051241.
6. SALOPEK ČUBRIĆ, I., SKENDERI, Z. Impact of cellulose materials finishing on heat and water vapour resistance. *Fibres & Textiles in Eastern Europe*, 2013, **97**(1), 61–66.
7. BOZSAKY, D. The historical development of thermal insulation materials. *Periodica Polytechnica Architecture*, 2010, **41**(2), 49–56, doi: 10.3311/pp.ar.2010-2.02.
8. DHANGAR, M., CHATURVEDI, K., MILI, M., PATEL, S. S., KHAN, M. A., BHARGAW, H. N. SRIVASTAVA, A. K., VERMA, S. Emerging 3D printed thermal insulating materials for sustainable approach: A review and a way forward. *Polymers for Advanced Technologies*, 2023, **34**(5), 1425–1434, doi: 10.1002/pat.5989.
9. GIBSON, P. W., LEE, C., KO, F., RENEKER, D. Application of nanofiber technology to nonwoven thermal insulation. *Journal of Engineered Fibers and Fabrics*, 2007, **2**(2), 32–40, doi: 10.1177/155892500700200204.
10. GRABOWSKA, B., KASPERSKI, J. The thermal conductivity of 3D printed plastic insulation materials – the effect of optimizing the regular structure of closures. *Materials*, 2020, **13**(19), 1–15, doi: 10.3390/ma13194400.
11. ZDRAVEVA, E., FANG, J., MIJOVIĆ, B., LIN, T. Electrospun nanofibers. In *Structure and Properties of High-performance Fibers*. Edited by Gajanan Bhat. Cambridge : Woodhead Publishing, 2017, 267–300, doi: 10.1016/B978-0-08-100550-7.00011-5.
12. SUKIGARA, S., GANDHI, M., AYUTSEDE, J., MICKLUS, M., KO, F. Regeneration of *Bombyx mori* silk by electrospinning – part 1: processing parameters and geometric properties. *Polymer*, 2003, **44**(19), 5721–5727, doi: 10.1016/S0032-3861(03)00532-9.
13. MIT-UPPATHAM, C., NITHITANAKUL, M., SUPAPHOL., P. Ultrafine electrospun polyamide-6 fibers: effect of solution conditions on morphology and average fiber diameter. *Macromolecular Chemistry and Physics*, 2004, **205**(17), 2327–2338, doi: 10.1002/macp.200400225.
14. BUCHKO, C.J., CHEN, L.C., SHEN, Y., MARTIN, D.C. Processing and microstructural characterization of porous biocompatible protein polymer thin films. *Polymer*, 1999, **40**(26), 7397–7407, doi: 10.1016/S0032-3861(98)00866-0.
15. YUAN, X., ZHANG, Y., DONG, C., SHENG, C. Morphology of ultrafine polysulfone fibers prepared by electrospinning. *Polymer International*, 2004, **53**(11), 1704–1710, doi: 10.1002/pi.1538.
16. TAN, S.-H., INAI, R., KOTAKI, M., RAMAKRISHNA, S. Systematic parameter study for ultra-fine fiber fabrication via electrospinning process. *Polymer*, 2005, **46**(16), 6128–6134, doi: 10.1016/j.polymer.2005.05.068.
17. LEE, D., JUNG, J., LEE, G. H., LEE, W. I. Electrospun nanofiber composites with micro-/nano-particles for thermal insulation. *Advanced Composite Materials*, 2019, **28**(2), 193–202, doi: 10.1080/09243046.2018.1478607.
18. CHEN, W., FU, M., WENG, W. Electrospinning of continuous nanofiber hollow yarns for thermal storage and insulation by a multi-step twisting method. *Textile Research Journal*, 2020, **90**(9–10), 1045–1056, doi: 10.1177/0040517519886023.

19. BAE, M., AHN, H., KANG, J., CHOI, G., CHOI, H. Determination of the long-term thermal performance of foam insulation materials through heat and slicing acceleration. *Polymers*, 2022, **14**(22), 1–18, doi: 10.3390/polym14224926.
20. MERILLAS, B., VILLAFAÑE, F., RODRÍGUEZ-PÉREZ, M.Á. Improving the insulating capacity of polyurethane foams through polyurethane aerogel inclusion: from insulation to superinsulation. *Nanomaterials*, 2022, **12**(13), 1–19, doi: 10.3390/nano12132232.
21. YOON, J.W., PARK, Y., KIM, J., PARK, C.H. Multi-jet electrospinning of polystyrene/polyamide 6 blend: thermal and mechanical properties. *Fashion and Textiles,* 2017, **4**(9), 1–12, doi: 10.1186/s40691-017-0090-4.
22. SABANTINA, L., HES, L., MIRASOL, J.R., CORDERO, T., EHRMANN, A. Water vapor permeability through PAN nanofiber mat with varying membrane-like areas. *Fibres & Textiles in Eastern Europe*, 2019, **1**(133), 12–15, doi: 10.5604/01.3001.0012.7502.
23. YAMAGUCHI, T., KUROKI, H., MIYATA, F. DMFC performances using a pore-filling polymer electrolyte membrane for portable usages. *Electrochemistry Communications*, 2005, **7**(7), 730–734, doi: 10.1016/j.elecom.2005.04.030.
24. ISO 11092:1993 Textiles – physiological effects – measurement of thermal and water-vapour resistance under steady-state conditions (sweating guarded-hotplate test). Geneva : International Organization for Standardization, 1993, 1–10.
25. SALOPEK ČUBRIĆ, I., SKENDERI, Z., MIHELIĆ-BOGDANIĆ, A., ANDRASSY, M. Experimental study of thermal resistance of knitted fabrics. *Experimental Thermal and Fluid Science*, 2012, **38**, 223–228, doi: 10.1016/j.expthermflusci.2011.12.010.
26. KIM, G.-T., HWANG, Y.-J., AHN, Y.-C., SHIN, H.-S., LEE, J.-K., SUNG, C.-M. The morphology of electrospun polystyrene fibers. *Korean Journal of Chemical Engineering*, 2005, **22**, 147–153, doi: 10.1007/BF02701477.
27. ANJUM, S., RAHMAN, F., PANDEY, P., ARYA, D.K., ALAM, M., RAJINIKANTH, P.S., AO, Q. Electrospun biomimetic nanofibrous scaffolds: a promising prospect for bone tissue engineering and regenerative medicine. *International Journal of Molecular Sciences*, 2022, **23**(16), 1–33, doi: 10.3390/ijms23169206.
28. LEE, S., OBENDORF, S.K. Transport properties of layered fabric systems based on electrospun nanofibers. *Fibers and Polymers*, 2007, **8**, 501–506, doi: 10.1007/BF02875872.
29. ZDRAVEVA, E., MIJOVIĆ, B. Parameters dependence of fibers diameter and pores area in electrospinning. *Advanced Engineering Forum*, 2018, **26**, 67–73, doi: 10.4028/www.scientific.net/AEF.26.67.
30. CAO, X., CHEN, W., ZHAO, P., YANG, Y., YU, D.-G. Electrospun porous nanofibers: pore–forming mechanisms and applications for photocatalytic degradation of organic pollutants in wastewater. *Polymers*, 2022, **14**(19), 1–25, doi: 10.3390/polym14193990.
31. DEMIR, M.M., YILGOR, I., YILGOR, E., ERMAN, B. Electrospinning of polyurethane fibers. *Polymer*, 2002, **43**(11), 3303–3309, doi: 10.1016/S0032-3861(02)00136-2.
32. SENCADAS, V., CORREIA, D.M., AREIAS, A., BOTELHO, G., FONSECA, A., NEVES, I., RIBELLES, J. G., MENDEZ, S. L. Determination of the parameters affecting electrospun chitosan fiber size distribution and morphology. *Carbohydrate Polymers*, 2012, **87**(2), 1295–1301, doi: 10.1016/j.carbpol.2011.09.017.
33. RIBEIRO, C., SENCADAS, V., COSTA, C. M., RIBELLES, J.L.G., LANCEROS-MÉNDEZ, S. Tailoring the morphology and crystallinity of poly (L-lactide acid) electrospun membranes. *Science and Technology of Advanced Materials*, 2011, **12**(1), 1–10, doi: 10.1088/1468-6996/12/1/11660947.

34. TORNELLO, P.R.C., CARACCIOLO, P.C., ROSELLÓ, J.I.I., ABRAHAM, G.A. Electrospun scaffolds with enlarged pore size: porosimetry analysis. *Materials Letters*, 2018, **227**, 191–193, doi: 10.1016/j.matlet.2018.05.072.
35. SCHREUDER-GIBSON, H., GIBSON, P., SENECAL, K., SENNETT, M., WALKER, J., YEOMANS, W. Protective textile materials based on electrospun nanofibers. *Journal of Advanced Materials*, 2002, **34**(3), 44–55.
36. OĞLAKCIOĞLU, N., AKDUMAN, C., SARI, B. Investigation of thermal comfort properties of electrospun thermoplastic polyurethane fiber coated knitted fabrics for wind-resistant clothing. *Polymer Engineering & Science*, 2021, **61**(3), 669–679, doi: 10.1002/pen.25607.
37. NASOURI, K., SHOUSHTARI, A.M., HAJI, A. The role of nanofibers diameter in the enhanced thermal conductivity of electrospun nanofibers. In *Proceedings of the The 6th TEX TEH International Conference*, *Bucharest, Romania*, 2013, 1–9.
38. ÖZKAN, E.T., KAPLANGIRAY, B.M. Investigating thermophysiological comfort properties of polyester knitted fabrics. *Journal of Textile Engineering & Fashion Technology*, 2019, **5**(1), 50–56, doi: 10.15406/jteft.2019.05.00180.
39. LU, X., WU, S. Thermo-physiological comfort properties of different woven fabrics used in sportswear for outdoor activities. *Thermal Science*, 2022, **26**(3B), 2707–2712, doi: 10.2298/TSCI2203707L.
40. MIJOVIĆ, B., SKENDERI, Z., SALOPEK ČUBRIĆ, I. Measurement of thermal parameters of skin-fabric environment. *Periodicum Biologorum*, 2010, **112**(1), 69–73.

Appendix

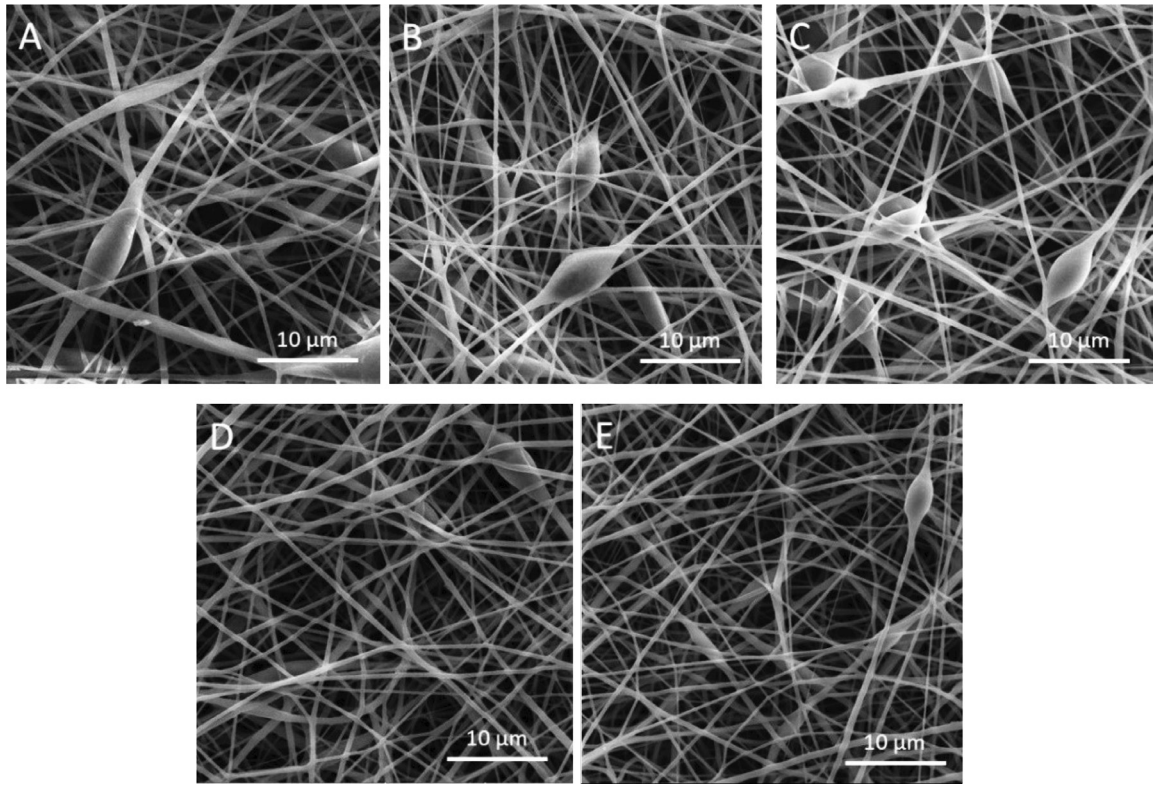

Figure A1: Electrospun 10 wt% PU at the electrical voltages of: a) 10 kV, b) 12 kV, c) 14 kV, d) 16 kV and e) 18 kV

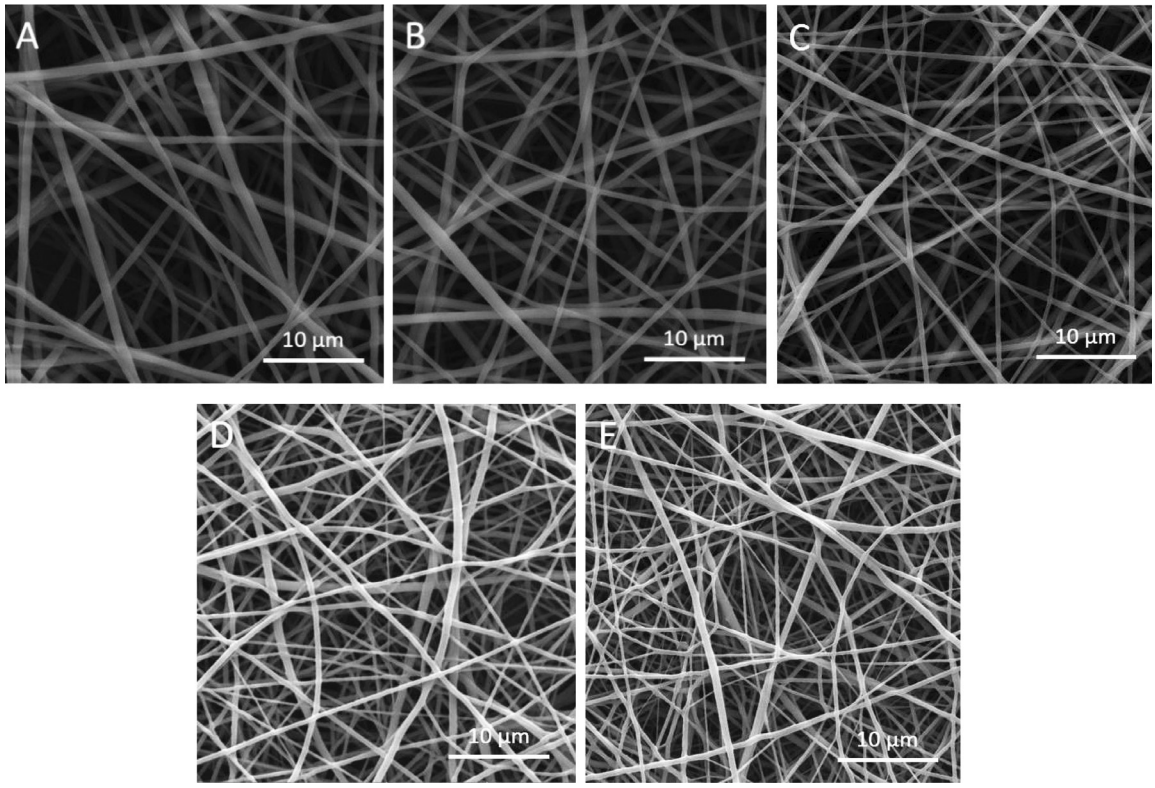

Figure A2: Electrospun 12 wt% PU at the electrical voltages of: a) 10 kV, b) 12 kV, c) 14 kV, d) 16 kV and e) 18 kV

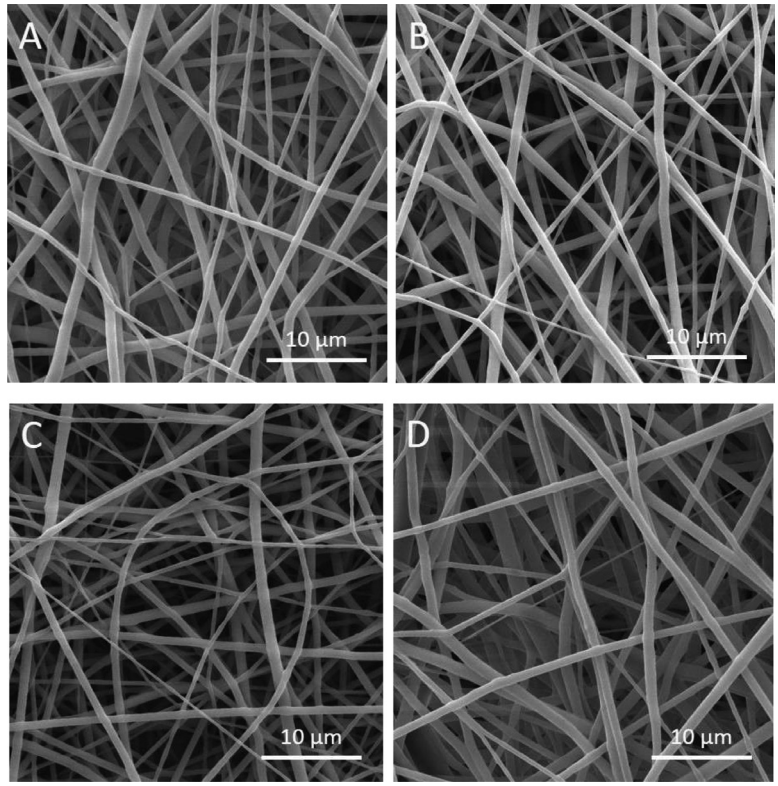

Figure A3: Electrospun 14 wt% PU at the electrical voltages of: a) 10 kV, b) 12 kV, c) 14 kV and d) 16 kV

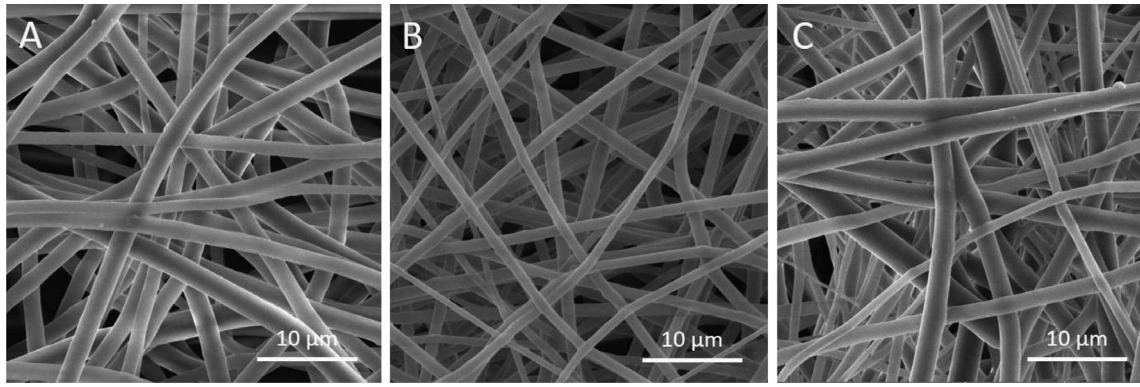

Figure A4: Electrospun 16 wt% PU at the electrical voltages of: a) 10 kV, b) 12 kV and c) 14 kV

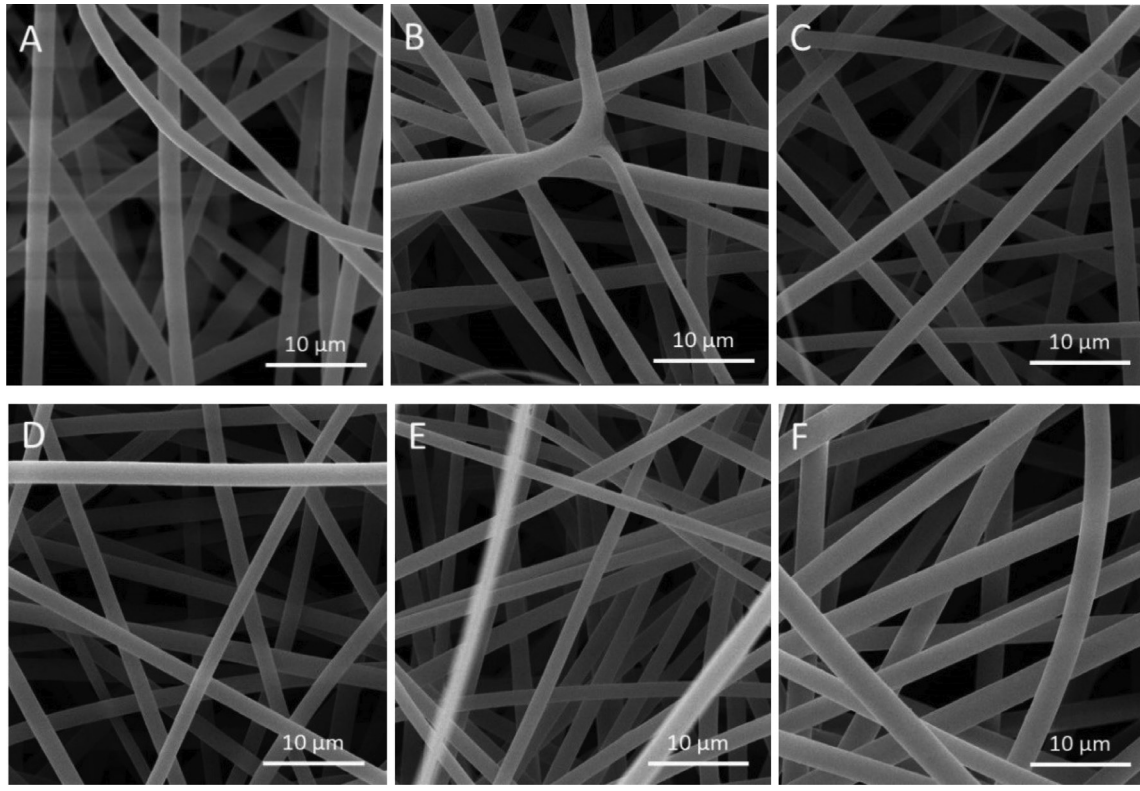

Figure A5: Electrospun 24 wt% PS at the electrical voltages of: a) 10 kV, b) 12 kV, c) 14 kV, d) 16 kV, e) 18 kV and f) 20 kV

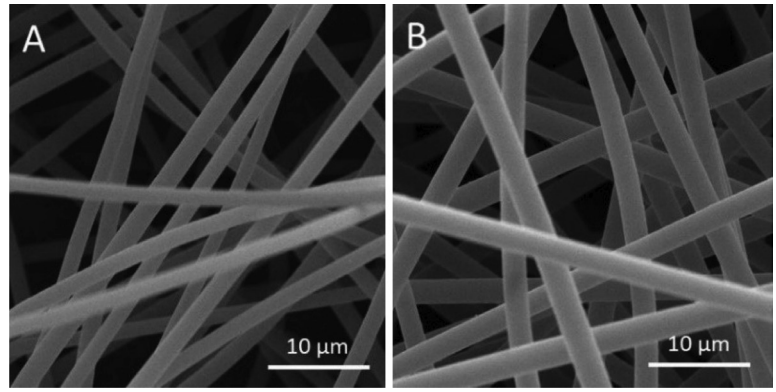

Figure A6: Electrospun 26 wt% PS at the electrical voltages of: a) 10 kV and b) 12 kV

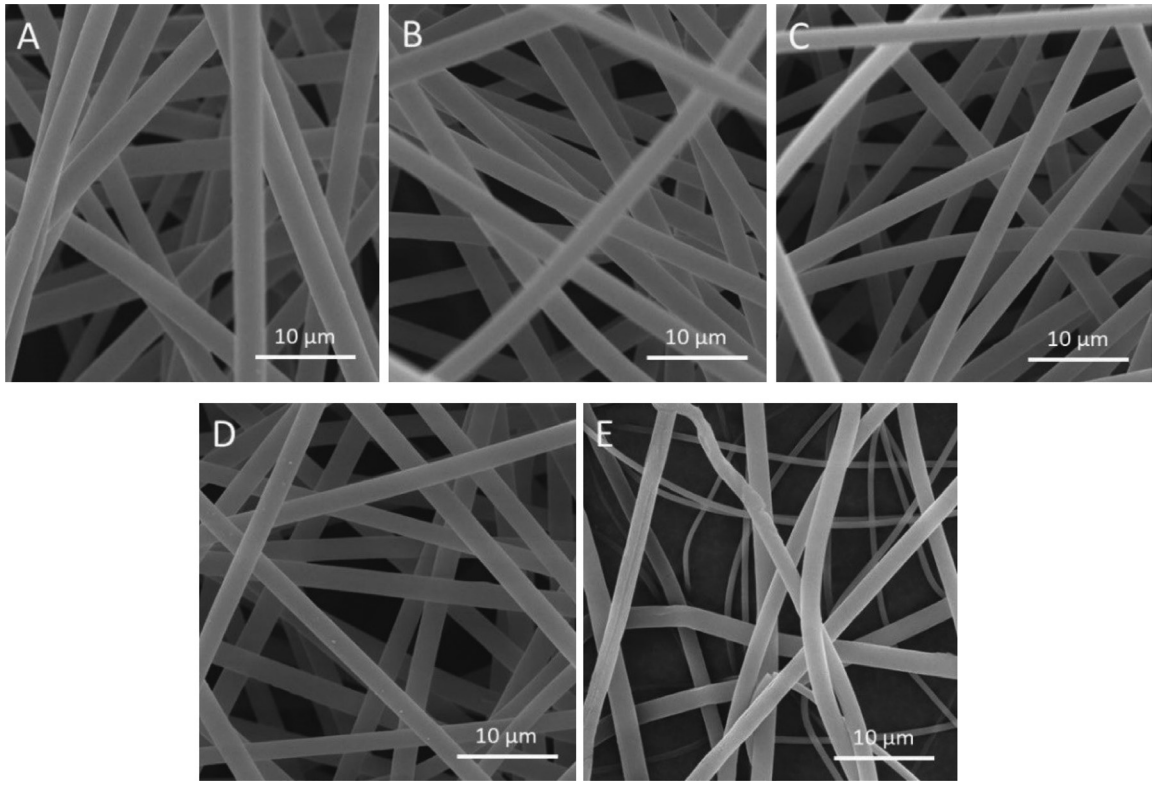

Figure A7: Electrospun 28 wt% PS at the electrical voltages of: a) 10 kV, b) 12 kV, c) 14 kV, d) 16 kV and e) 18 kV

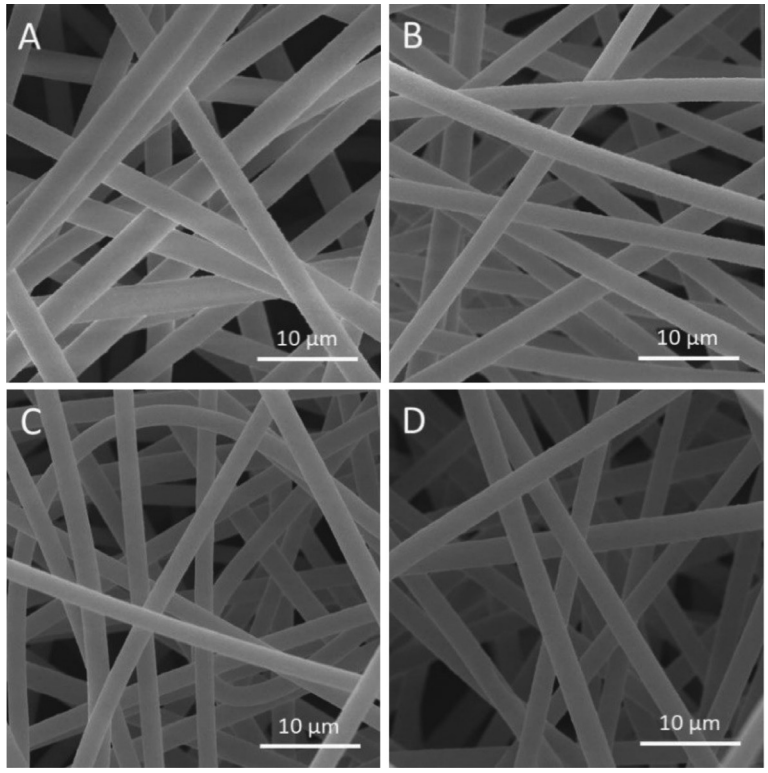

Figure A8: Electrospun 30 wt% PS at the electrical voltages of: a) 10 kV, b) 12 kV, c) 14 kV and d) 16 kV